

We are IntechOpen, the world's leading publisher of Open Access books Built by scientists, for scientists

6,900

Open access books available

185,000

International authors and editors

200M

Downloads

Our authors are among the

154

Countries delivered to

TOP 1%

most cited scientists

12.2%

Contributors from top 500 universities



WEB OF SCIENCE™

Selection of our books indexed in the Book Citation Index
in Web of Science™ Core Collection (BKCI)

Interested in publishing with us?
Contact book.department@intechopen.com

Numbers displayed above are based on latest data collected.
For more information visit www.intechopen.com



Neural Network Inverse Modeling for Optimization

Oscar May , Luis J. Ricalde , Bassam Ali ,
Eduardo Ordoñez López ,
Eduardo Venegas-Reyes and Oscar A. Jaramillo

Additional information is available at the end of the chapter

<http://dx.doi.org/10.5772/63678>

Abstract

In this chapter, artificial neural networks (ANNs) inverse model is applied for estimating the thermal performance (η) in parabolic trough concentrator (PTC). A recurrent neural network architecture is trained using the Kalman Filter learning from experimental database obtained from PTCs operations. Rim angle (ϕ_r), inlet (T_{in}), outlet (T_{out}) fluid temperatures, ambient temperature (T_a), water flow (F_w), direct solar radiation (G_b) and the wind velocity (V_w) were used as main input variables within the neural network model in order to estimate the thermal performance with an excellent agreement ($R^2=0.999$) between the experimental and simulated values. The optimal operation conditions of parabolic trough concentrator are established using artificial neural network inverse modeling. The results, using experimental data, showed that the recurrent neural network (RNN) is an excellent tool for modeling and optimization of PTCs.

Keywords: solar concentrating, thermal efficiency, neural networks, Kalman training optimization, solar energy

1. Introduction

About 80% of the energy consumed worldwide come from conventional energy sources, where more than 50% is used by the industry being a large part of this demand for the generation of heat industrial process [1, 2]. However, the use of fossil fuels to satisfy this demand has led to severe environmental impacts, which together with the decline of this resource has led to global energy policies focus on replacing fossil fuels with sustainable energy sources. The use of solar thermal systems could help to reduce CO₂ emissions and other pollutants in the atmosphere.

Solar energy is one of the renewable energies that attract more attention due to its abundance, cleanliness, and the fact that it does not generate any pollution [3]. On the other hand, in the industries exist several processes that require thermal energy with temperature range between 60 and 250 °C for heat process generation; industries such as dairies, plastics, canned food, textile, paper, etc. employ this kind of energy to process such as drying, sterilizing, cleaning, evaporation, steam and conditioning warehouses space for both heating and cooling [4]. This energy could be easily supplied by solar collectors using photothermal conversion. The thermal storage process is used to supply the required power loading when there is no sunlight. Amongst the middle-temperature solar collectors are the parabolic trough, Fresnel, compound parabolic collectors (CPCs) and evacuated tubes. In this work, we consider parabolic trough solar concentrators (PTCs) that could yield the heat within the temperature between 90 and 400 °C. Parabolic trough solar concentrators (PTCs) are one of the most mature technologies developed in this area [5]. Nevertheless, the use of this technology entails certain difficulties because of a large number of operational and environmental parameters. This becomes an extremely complicated study on these systems, creating complex nonlinear equations for compression, which results in the employment of sophisticated control systems to operate and optimize the PTC performance, in order to maximize its cost-benefit during the operation. The modeling and simulation of these systems should take into account the collector, the thermal load, and the losses to the environment and the power auxiliary supply.

In the last decades, in the area of renewable energy, the employ of computational intelligence methods such as artificial neural networks (ANN) has been rising to perform modeling and optimization process [6] because all the information based on renewable energy systems is very volatile and it has too much noise and also the behavior does not present a linear trend. In recent years, one of the most promising approaches for modeling and control of the highly nonlinear processes is the use of recurrent neural network. For most applications on time series forecasting, recurrent neural network (RNN) using the back-propagation learning algorithm has presented good results. However, this learning law is based on the gradient descent method and its convergence speed could not meet the requirements when fast responses are needed. Another well-known training algorithm is the Levenberg-Marquardt whose main disadvantage is that it does not guarantee finding the global minimum and its learning speed could be slow since it depends on the initialization values. To overcome the learning speed and uncertainties issues, recently, the extended Kalman Filter (EKF)-based algorithms have been implemented to train neural networks. With the EKF-based algorithm, the learning convergence is improved [6]. Using the EKF training on recurrent neural networks drives to improve results mostly in control, identification and predictions applications where the critical variables are subject to uncertainties and unmodeled dynamics. However, the EKF training requires the heuristic selection of some design parameters, which is not always an easy task.

This chapter is focused on presenting the methodology used to conduct the process of modeling the thermal efficiency of an array of PTCs, in order to bring the system to optimal operating conditions through a desired efficiency by using ANN. The chapter is divided into five sections: Section 2 describes the experimental system composed by parabolic trough solar concentrations; Section 3 details the artificial neural network as modeling tool; Section 5

presents the development of the inverse modeling for optimization; and Section 6 describes the conclusions.

2. Experimental system: parabolic trough solar concentrations

2.1. Experiment description

The experimental system corresponds to a low enthalpy steam generation plant built according to the ASHRAE 93-1986 (RA 91) standard [7]; it is composed by:

- three PTCs (with 90° rim angle) with a length of 2.44 m and an aperture of 1.06 m;
- two storage thermic tanks of 120 L capacity which cover two functions: the first is to preheat the water for the characterization of PTC employing electrical resistances inside the tanks (the first with 3 kW and second with 6 kW) and the second is to store the energy produced by PTCs;
- a hydraulic circuit and two centrifugal water pumps of ½ HP is employed to recirculate the preheated water to PTCs and then return it to the tanks;
- a set of sensors consisting in a Hedland HB2800 flow meters, pressure and temperature meters at the storage thermic tanks outlet, such as pressure and temperature meters at the outlet of PTCs.

For the measurement of environmental conditions, a pyranometer, an anemometer and temperature sensors were employed. **Figure 1** shows the diagram of the experimental system.

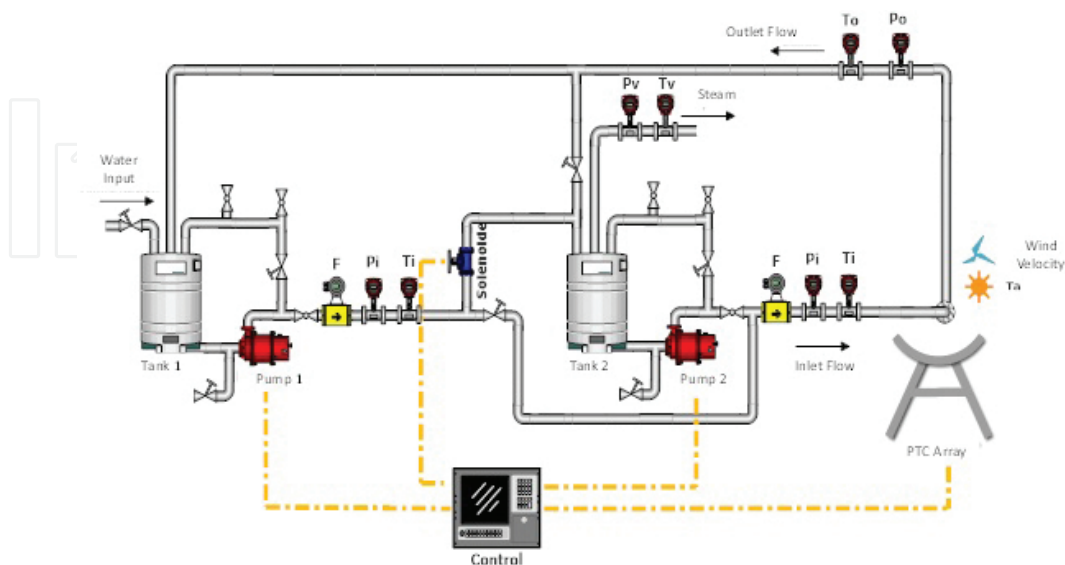


Figure 1. Operation diagram of parabolic solar concentration experimental system.

2.2. Performance of parabolic trough solar collector (PTC)

A parabolic trough solar concentrator consists of a shaped channel sheet with parabolic cross-section whose surface must have a high reflectance value (ρ); at the focus of parabola (f) is situated an absorber metal tube covered with a selective surface with high absorptivity (α) and low emissivity (ϵ). A glass tube with high transmissivity (τ) is placed concentric to the absorber to minimize the convective losses; in the same way, the space between both tubes must be evacuated to avoid the conduction losses. Inside the absorber tube, the working fluid gains energy due to the concentration of solar irradiation at the focal line resulting in the temperature increase of the working fluid [8]. **Figure 2** shows cross-section of a PTC.

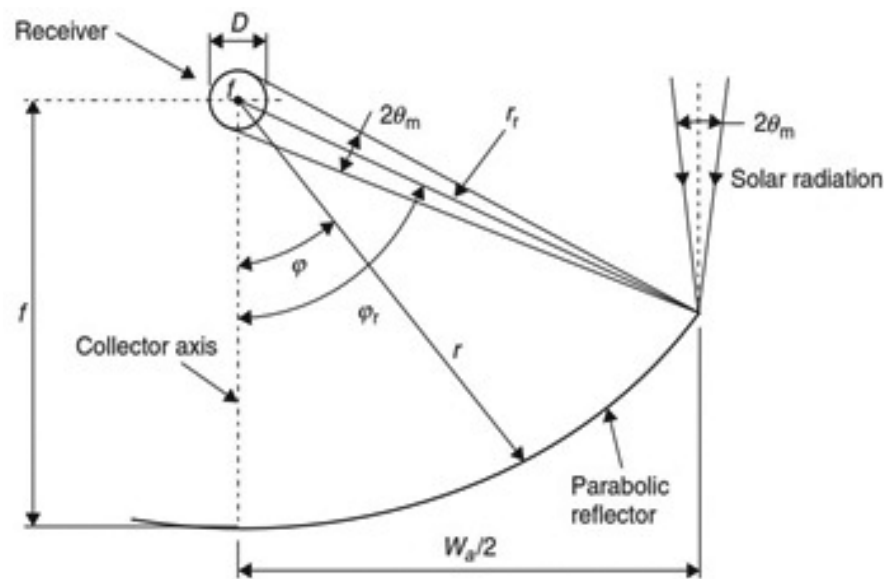


Figure 2. Parabolic trough solar concentrator.

Rim angle (ϕ_r)	a	B	c
40°	2	1.5795	1.4927
50°	2	1.7404	1.5199
60°	18	14.420	5.6055
70°	2	2.3000	1.5974
80°	2	2.7846	1.6485
90°	2	2.8284	2.4142

Table 1. Constant values respect the rim angle.

One of the most practical ways to calculate the dimensions of a PTC by considering the curve length S of the reflective surface is given by:

$$S = \frac{f}{a} \left(b - \frac{a}{2} \ln(f^2) + a \ln(cf) \right) \quad (1)$$

where the coefficients a , b and c are determinates by the angle that form the parabolic surface with respect to the focal line which is called rim angle (ϕ_r). **Table 1** shows the values of this these coefficients for different rim angles.

Another important parameter related to the rim angle (ϕ_r) is the aperture of the parabola (W_a). From **Figure 2** and simple trigonometry, it can be found [9] that:

$$W_a = 4f \tan(h_p/2) \quad (2)$$

where h_p is the latus rectum of the parabola.

2.2.1. Optical performance

The optical efficiency (η_o) of a PTC is defined as the ratio of solar energy that falls on the surface of the absorber tube and that which falls on the reflective surface of the collector. It is commonly given as [10]:

$$\eta_o = \rho\tau\alpha\gamma \left[(1 - A_f \tan(\theta)) \cos(\theta) \right] \quad (3)$$

where θ is the factor intersection receptor, θ is the sun rays incident angle and A_f is the ratio of the area of loss and opening area of the PTC (called geometric factor).

There are two types of errors associated with the parabolic surface: random and no random. The first type of errors is apparent changes in the sun width, scattering effects caused by random slope errors and associated with the reflective surface; these can be represented by normal probability distributions. The second class of errors depends on the manufacturing and operation of the collector. These errors are due to the reflector profile imperfections, misalignment and receiver location errors [11]. Random errors are modeled statistically to calculate the standard deviation of the distribution of the total energy reflected at normal incidence [12]:

$$\sigma_{\text{Tot}} = \sqrt{\sigma_{\text{sol}}^2 + 4\sigma_{\text{pend}}^2 + \sigma_{\text{ref}}^2} \quad (4)$$

where σ_{sol} is the standard deviation of the distribution of solar form, σ_{pend} is the standard deviation of the slope errors and σ_{ref} is the standard deviation of the distribution of the errors of the reflective surface.

2.2.2. Thermal performance

The experimental evaluation for thermal performing of PTC is realized according to the ASHRAE 93-1986 (RA 91) standard [7]. This standard provides a widely known method to obtain the thermal efficiency of solar energy collector that uses single phase fluids, in order to

be compared with the similar solar collectors [13]. Therefore according to the standard, the thermal instantaneous efficiency (η_g) on a PTC is evaluated experimentally by considering:

$$\eta_g = \frac{m' C_p (T_o - T_i)}{(A_a G_b)} \quad (5)$$

where T_i and T_o are the inlet and outlet temperatures, respectively, m' is the mass flow rate, C_p is the specific heat, A_a is the aperture area of the collector and G_b is the direct solar irradiation component in the aperture plane of the collector. To avoid the phase change in the water that is used as thermal fluid, T_i is restricted between 20 and 90°C.

On the other hand, the PTC thermal efficiency (η_T) employing the first law of thermodynamic is given by [8]:

$$\eta_T = F_R \left[\eta_o - \frac{U_L}{C_o} \left(\frac{\Delta T}{G_b} \right) \right] \quad (6)$$

where ($\Delta T = T_i - T_a$) is the temperature rise across the receiver, and T_a is the environmental temperature. As can be seen, Eq. (6) has the form of an equation of line, where $F_R U_L / C_o$ represents the pediment and $F_R \eta_o$ represents the interception. This relation can be applied to obtain experimentally the heat removal factor F_R and the overall heat loss coefficient U_L for a PTC.

3. Artificial neural network as modeling tool

3.1. Artificial recurrent neural networks

Artificial neural networks (ANN) are adaptive systems developed in the form of computational algorithms or electric circuits, which are inspired in the biological neuron system operation. An ANN is composed of a large number of interconnected units called neurons that have a certain natural tendency for learning information from the outside world [14]. These structures are used to estimate or approximate functions that may depend on a lot of variables, which are generally unknown reason for why the ANN have been used in many practical applications such as pattern recognition, estimation of series time and modeling of nonlinear processes [15].

A model of ANN can be seen as a black box to which is entered a database composed of a series of input variables; each of these input variables is assigned an appropriate weighting factor called weight (W). The sum of the weighted inputs and the use of bias (b) for adjustment produce an input value applied to a transfer function to generate an output (**Figure 3**). The main feature of these models is that they do not require specific information on the physical behavior of the system or how they were obtained data [16].

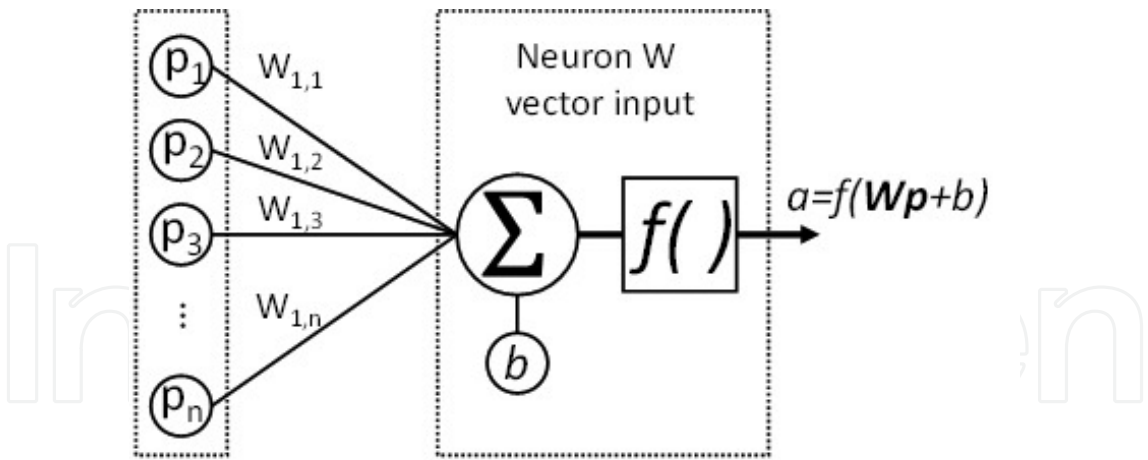


Figure 3. Artificial neuron with n inputs.

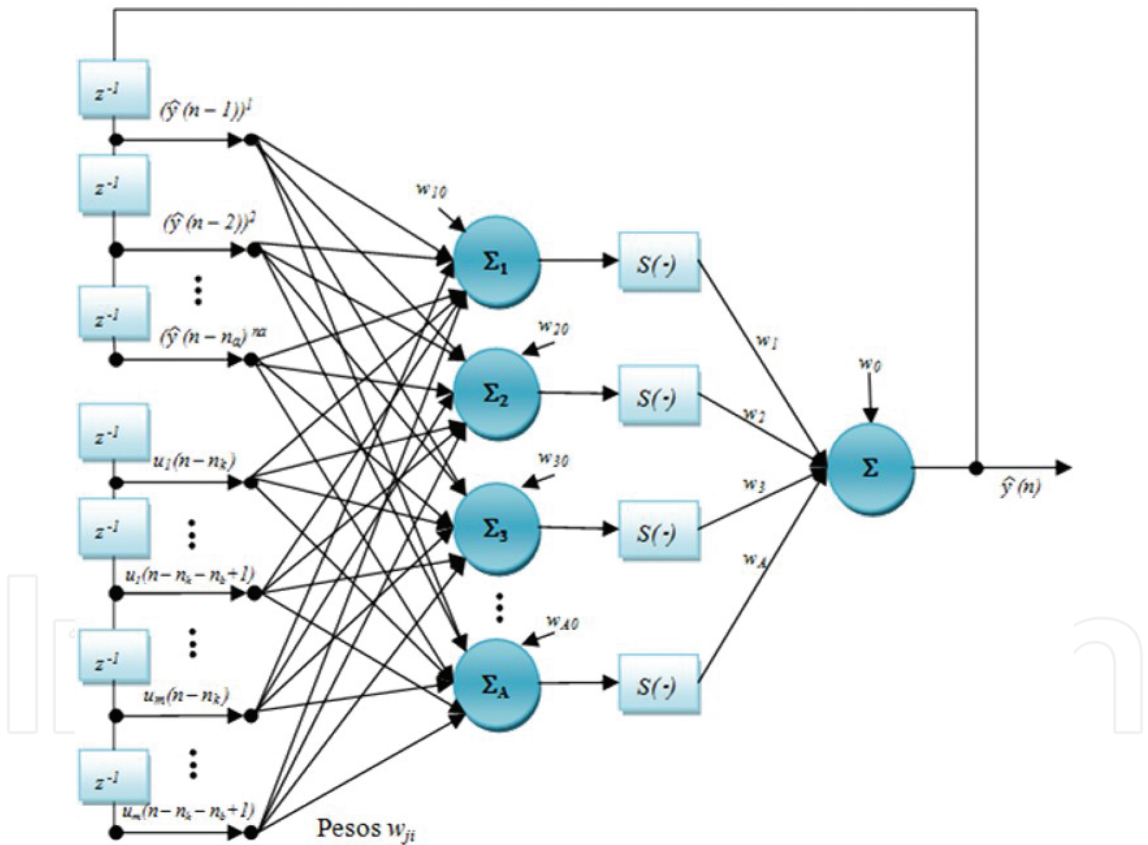


Figure 4. Recurrent neural network.

Among the many existing ANN models the most widely used is known as multi-layer perceptron (MLP) [17], which is used to solve multivariable problems by nonlinear equations using a process called training. The training process is performed through specific learning algorithms, where the most widely used is known as back-propagation through time [18]. The

architecture of an MLP is usually divided into three parts known as: input layer, hidden layer and output layer. During the training process, the MLP learns from past errors to get a model that describes as closely as possible to the nonlinear phenomenon. To carry out this, during the training phase they adapt the weight and bias parameters until the approximation error is minimized [19].

A recurrent neural network responds temporally to an external input signal where the feedback allows the RNN to have a representation in state space; this versatility makes them convenient for diverse applications for modeling, optimization and control. The order in an RNN refers to the form in which the neuron activation potential is defined [20]. When the local activation potential is combined with products of signals coming from the feedback or when products are made between the later and the external input signals to the network, a neural network of order emerges, where the order represents the number of signals that are multiplied. In this work, in order to carry out modeling of the process, a high order recurrent neural network is designed. The structure is composed by an input vector, one hidden layer and an output layer composed of just one neuron with a linear activation function. In **Figure 4**, the designed recurrent neural network architecture is depicted.

According to **Figure 4**, $\rho_i(k)$ is the input i to the neural network, $v_j(k)$ is the neuron j activation potential, $y_j(k)$ represents the neuron j output, $v(k)$ is the output neuron activation potential, $\hat{y}(k)$ is the neuron output in the output layer (neural network output), $\phi(v_j(k))$ represents the neuron j activation function, $\phi(v(k))$ is the activation function of the output layer neuron, $w_{ji}(k)$ is the weight connecting the input i to the neuron j input, $w_j(k)$ is the weight connecting neuron j output to the neuron input in the output layer, and s and A are the inputs total number to the neurons in the hidden and output layers, respectively.

For the set of weights, we construct a weight vector that will be estimated by means of the Kalman Filtering. The Kalman Filtering (KF) algorithm was first designed as a method to estimate the state of a system under noise on the process and on the measurement. Consider a linear, discrete-time dynamical system described by

$$w(k+1) = F_{k+1,k} w(k) + v_1(k) \quad (7)$$

$$y(k) = H(k)w(k) + v_2(k) \quad (8)$$

Eq. (7) is known as the process equation; $F_{k+1,k}$ is the transition matrix taking the state $w(k)$ from iteration k to iteration $k+1$ and $v_1(k)$ is the process noise. On the other hand, Eq. (8) is known as the output measurement, which represents $y(k)$ i.e. the observable part of the state at iteration k , $H(k)$ is the measurement matrix and $v_2(k)$ is the measurement noise. Both the process noise $v_1(k)$ and the measurement noise $v_2(k)$ are assumed as white noise with covariance matrices given by $E[v_1(l)v_1^T(l)] = \delta_{k,l}Q(k)$ and $E[v_2(l)v_2^T(l)] = \delta_{k,l}R(k)$. To deal with the nonlinear structure of the recurrent neural network mapping, an EKF algorithm is developed. The learning algorithm for the recurrent neural network based on the EKF is described as

$$K(k) = P(k)H^T(k)[R + H(k)P(k)H^T(k)]^{-1}, w(k+1) = w(k) + K(k)[y(k) - \hat{y}(k)], P(k+1) = P(k) - K(k)H(k)P(k) + Q \quad (9)$$

where $P(k)$ and $P(k+1)$ are the prediction error covariance matrices, $w(k)$ is the neural weight vector, $y(k)$ is the measured output vector, $\hat{y}(k)$ is the neural network output, $K(k)$ is the Kalman gain matrix, and Q and R are the state and measurement noise covariance matrices. The matrices P , Q and R are assumed to be diagonal and are initialized using random values P_0 , Q_0 and R_0 , respectively.

The $H(k)$ matrix is defined with each derivative of one of the neural network output, (y_i), with respect to one neural network weight, (w_j), as follows:

$$H_{ij}(k) = \left. \frac{\partial \hat{y}_i(k)}{\partial w_j(k)} \right|_{w(k)=\hat{w}(k+1)} \quad i = 1, \dots, o; \quad j = 1, \dots, NW$$

where NW is the total number of neural network weights and o is the total number of outputs.

4. ANN inverse model

In order to solve the optimization problem proposed, a computational intelligence methodology is developed. The proposed approach is divided into two parts: first is the generation of a mathematical model by RNN and the second part is responsible for performing inverse neural network for the optimization process. **Figure 5** displays the methodology divided into three steps: (i) the first step consist in generate a database with the most important parameters

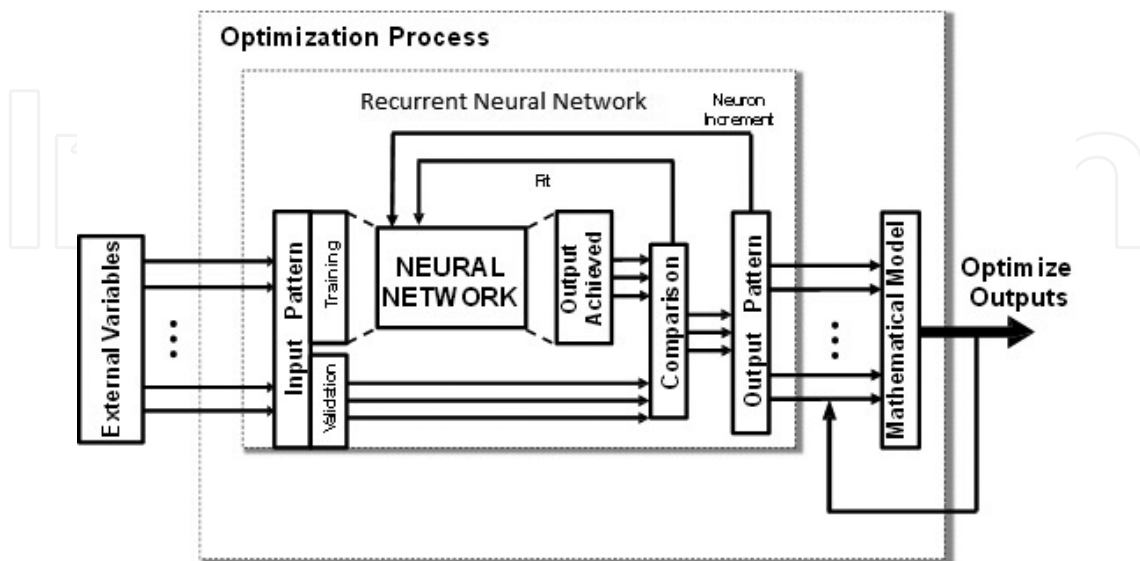


Figure 5. Optimization by neural network methodology.

that could affect the desired output, which is schematized in **Figure 6**, which in our case is the thermal efficiency, (ii) in the second step an RNN model is trained to obtain the best approximation error that relates the inputs with desirable outputs; (iii) in the last step one of the RNN inputs is selected to function as a control variable to perform the optimization process by an inverse neural network architecture.

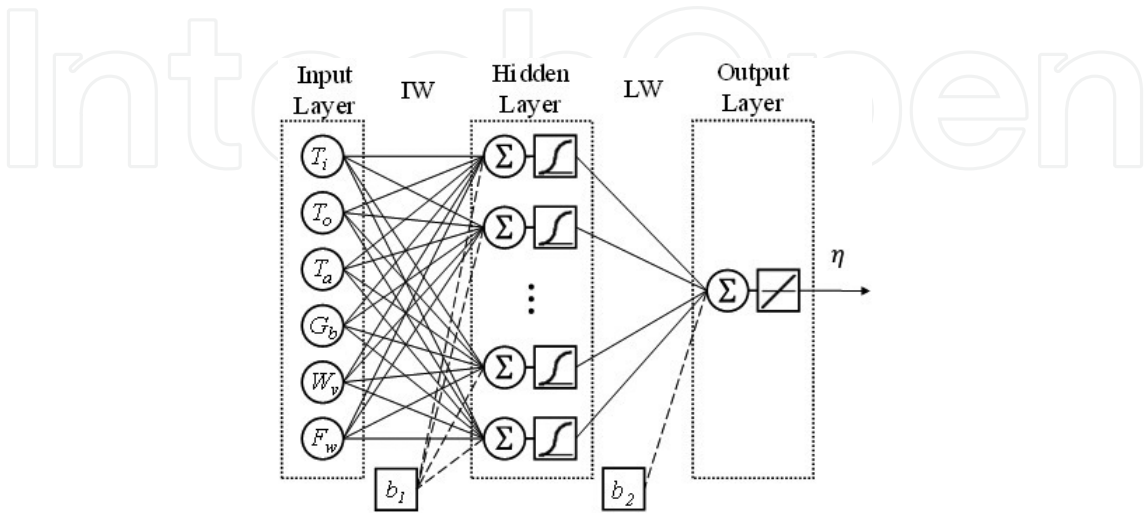


Figure 6. Neural network architecture for the mathematic model of thermal efficiency.

Parameters	Min	Max	Units
Input			
Operational variables			
Inlet flow temperature (T_{in})	27.75	86.30	[°C]
Outlet flow temperature (T_{out})	34.70	100.2	[°C]
Flow working fluid (F_w)	0.94	6.11	[L/min]
Environmental variables			
Ambient temperature (T_{amb})	24.26	33.99	[°C]
Direct solar radiation (G_b)	830.0	1014	[W/m²]
Wind velocity (V_w)	0.95	3.98	[m/s²]
Output			
Thermal efficiency (Eff)	0.16	0.63	[-]

Table 2. Parameters employed at the ANN prediction model.

Experimental database provided by Jaramillo et al. [13], consists of different η values calculated from the thermodynamic parabolic trough concentrator model (Eqs. (5) and (6)). The parameter measurements are divided into two categories: operational variables conformed by inlet

temperature (T_i) and outlet temperature (T_o) working fluid, as well as flow working fluid (F_w); and environmental variables composed by ambient temperature (T_a), direct solar radiation (G_b) and wind velocity (V_w). **Table 2** shows the six parameters that form the database and the minimum and maximum ranges of each one.

The development of predictive mathematical model of the experimental database was divided into two processes; the main process (in these case 80%) was destined to RNN learning and testing process and the other part (20%) was employed for the validation of the results, in order to obtain a good representation of the data distribution.

At the training process, a normalized database was entered into a MLP architecture, where the number of neurons at the input and output layers was given by the number of input and output variables in the process, respectively. The Kalman Filter training algorithm in Eq. (9) was employed to obtain the optimum weights and bias for the RNN model as the one displayed in **Figure 4**.

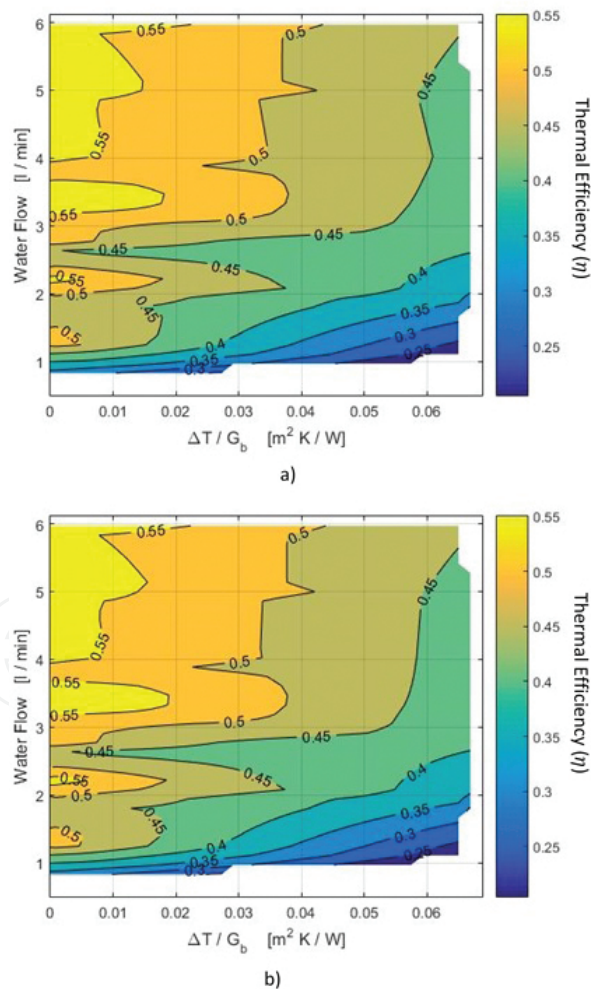


Figure 7. Thermal efficiency validation. (a) Experimental thermal efficiency not included at training and (b) simulate thermal efficiency from RNN model.

To validate the MLP model, a comparison was carried out employing the data not included in the training process. The output values comparison (thermal efficiency) was made in function of two variables, the heat loss parameter ($\Delta T/G_b$) and the working fluid flow. **Figure 7a** shows the real behavior of the thermal efficiency of the system in function of both parameters (heat loss parameter and fluid flow) and where can be seen a trend to decrease when ΔT increases [21]. Furthermore, **Figure 7b** represents the values of thermal efficiency obtained from the mathematical model generated with MLP where an appropriate reproduction of the real efficiency curves can be seen, demonstrating that the model is capable of adapting to the variations of flow and heat losses.

4.1. Optimization of the inverse artificial neural network

Once generated the desired mathematical model and proven effective, an optimization process is applied. To perform the optimization analysis, an input variable must be selected as control input. The selected variable in the present application was the water flow since it can be manipulated and quickly impact the system behavior. For the optimization process, the output generated by the ANN model (thermal efficiency) acts as input to a process modeled from experimental values, generating as output a control variable that minimizes the difference for the desired thermal efficiency. **Figure 8** displays the inverse ANN architecture.

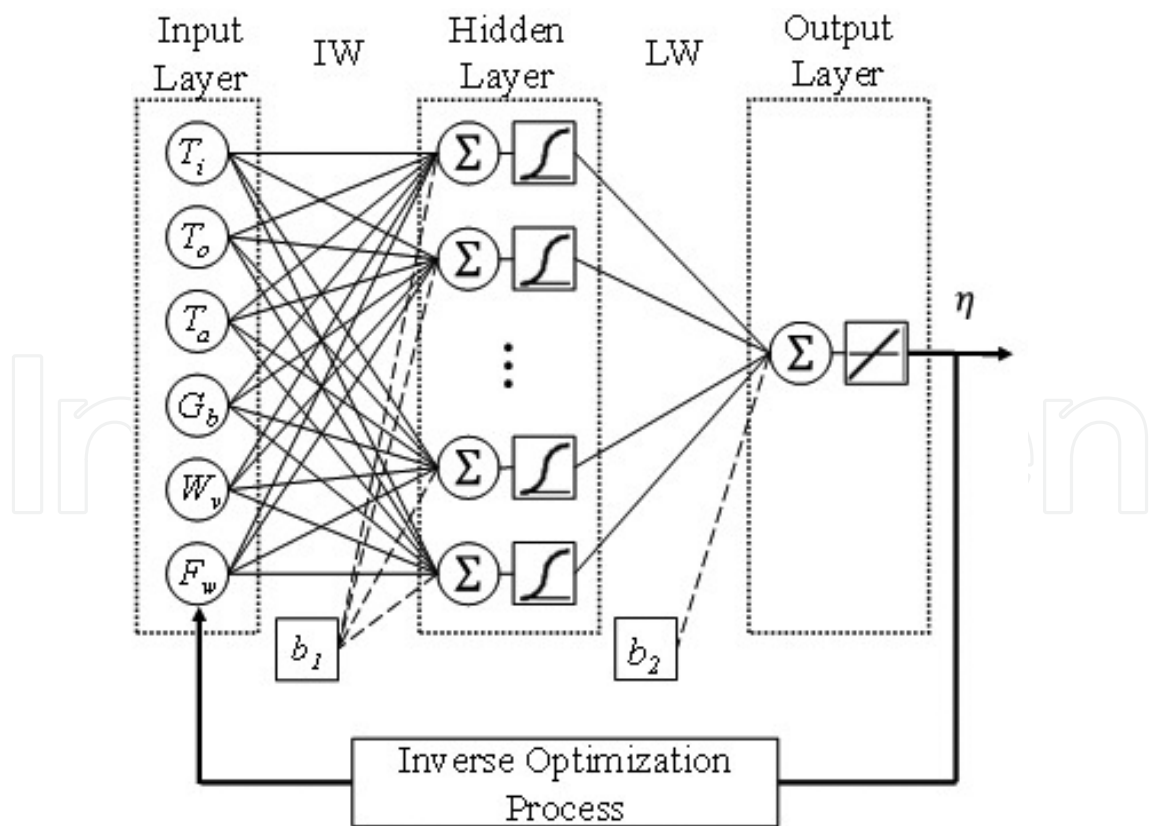


Figure 8. Inverse artificial neural network.

5. Conclusions

The aim of this chapter was to design an artificial neural network algorithm to predict the thermal performance of a parabolic trough concentrator, in order to develop a new approach for the estimation of the optimal operation condition of PTCs for a desired efficiency. A recurrent neural network was applied to model the nonlinear characteristics of the process with an excellent approximation of the thermal efficiency.

Author details

Oscar May¹, Luis J. Ricalde^{1*}, Bassam Ali¹, Eduardo Ordoñez López¹,
Eduardo Venegas-Reyes² and Oscar A. Jaramillo³

*Address all correspondence to: lricalde@correo.uady.mx

1 Universidad Autónoma de Yucatán, Facultad de Ingeniería, Av. Industrias no Contaminantes por Periférico Norte, Cordemex, Mérida, Yucatán, México

2 Investigador de Cátedras CONACYT, Centro de Investigación en Materiales Avanzados, Centro, Durango, México

3 Instituto de Energías Renovables, Universidad Nacional Autónoma de México, Privada Xochicalco s/n, Temixco, Morelos, México

References

- [1] Zou B., Dong J., Yao Y., Jiang Y., An experimental investigation on a small-sized parabolic trough solar collector for water heating in cold areas, *Applied Energy* 163, 396–407, 2016.
- [2] Fernández-García A., Rojas E., Pérez M., Silva R., Hernández-Escobedo Q., Manzano-Agugliaro F., A parabolic-trough collector for cleaner industrial process heat, *Journal of Cleaner Production* 89, 272–285, 2015.
- [3] Mekhilef S., Saidur R., Safar A., A review of solar energy use in industries, *Renewable and Sustainable Energy Reviews*, 1777–1790, 2011.
- [4] Venegas-Reyes E., Jaramillo O.A., Castrejón-García R., Aguilar J.O., Sosa-Montemayor F., Design, construction, and testing of a parabolic trough solar concentrator for hot water and low enthalpy steam generation. *Journal of Renewable Sustainable Energy* 4, 053103, 2012.

- [5] Lamba D.K., A review on parabolic trough type solar collectors: innovation, applications and thermal energy storage. *Proceedings of the National Conference on Trends and Advances in Mechanical Engineering*; 2011. pp. 90–99.
- [6] Sanchez E.N., Alanis A.Y., Rico J., Electric load demand prediction using neural networks trained by Kalman Filtering. *IEEE International Joint Conference on Neural Networks*, Budapest, Hungary; 2004. pp. 2771–2775.
- [7] ANSI/ASHRAE 93-1986 (RA 91). Methods of testing to determine the thermal performance of solar collectors. American Society of Heating, Refrigerating and Air-Conditioning Engineers, Inc.; 1991.
- [8] Kalogirou S., *Solar Energy Engineering: Processes and Systems*. USA: Academic Press; 2009. ISBN 978-0-12-374501-9.
- [9] Duffie J., Beckman W., *Solar Engineering of Thermal Processes*. New Jersey: Elsevier; 2013.
- [10] Valan-Arasu A, Sornakumar T., Design, manufacture and testing of fiberglass reinforced parabola trough for parabolic trough solar collectors. *Solar Energy* 81(10), 1273–1279, 2007.
- [11] Güven H.M., Bannerot R.B., Determination of error tolerances for the optical design of parabolic troughs for developing countries. *Solar Energy* 36, 535–550, 1986.
- [12] Rabl A., *Active Solar Collectors and their Applications*. New York, USA: Oxford University Press; 1984. ISBN 0-19-503546-1.
- [13] Jaramillo O.A., Venegas-Reyes E., Aguilar J.O., Castrejón-García R., Sosa Montemayor F., Parabolic trough concentrators for low enthalpy processes. *Renewable Energy* 60, 529–539, 2013.
- [14] Lippmann R.P., An introduction to computing with neural nets. *IEEE ASSP Magazine* 4(2), 4–22, 1987.
- [15] Haykin S., *Neural Networks*. 2nd ed. Prentice Hall, New Jersey, USA, 1999.
- [16] Bassam A., Conde-Gutierrez R. A., Castillo J., Laredo G., Direct neural network modeling for separation of linear and branched paraffins by adsorption process for gasoline octane number improvement. *Fuel* 124 (15) 158–167, 2014.
- [17] Rumelhart D., Geoffrey E., Williams R.J., Learning internal representations by error propagation. *Parallel distributed processing: explorations in the microstructure of cognition*, Volume 1: Foundations. MIT Press; MA, USA, 1986.
- [18] Demuth H., Beale M., *Neural Network Toolbox for Use with MATLAB, User's Guide Version 4*. The MathWorks, Natick, MA, USA, 2002.
- [19] Wasserman P., Schwartz T., Neural networks. II. What are they and why is everybody so interested in them now?. *IEEE Expert* 3(1), 10–15, 1988.

- [20] Sanchez E.N., Alanis A.Y., Loukianov A.G., Discrete-Time High Order Neural Control Trained with Kalman Filtering. Berlin, Germany: Springer-Verlag; 2008.
- [21] May O., Ali B., Flota M., Ordoñez E.E., Ricalde L., Quijano R., Vega A.E., Thermal efficiency prediction of a solar low enthalpy steam generating plant employing artificial neural networks communications in computer and information science – Volume 597. In: Anabel Martin-Gonzalez, A., Uc-Cetina, V., editors. Intelligent Computing Systems – First International Symposium, ISICS 2016, Mérida, México, March 16–18, 2016, Proceedings; 2016.

